Parvalbumin deficiency in fast-twitch muscles leads to increased 'slow-twitch type' mitochondria, but does not affect the expression of fiber specific proteins

Peter Racay*, Patrick Gregory and Beat Schwaller

Department of Medicine, Division of Histology and General Embryology, University of Fribourg, Switzerland

Keywords
calcium binding; E-F hand; fast twitch muscle; mitochondria; organelle biogenesis

Correspondence
B. Schwaller, Division of Histology, Department of Medicine, University of Fribourg, CH-1700 Fribourg, Switzerland
Fax: +41 26 3009732
Tel: +41 26 3008508
E-mail: Beat.Schwaller@unifr.ch

***Present address**
Comenius University, Jessenius Faculty of Medicine, Institute of Biochemistry, Mala Hora 4, SK-03601 Martin, Slovakia

doi:10.1111/j.1742-4658.2005.05046.x

Parvalbumin (PV), a small cytosolic protein belonging to the family of EF-hand calcium-binding proteins, is highly expressed in mammalian fast-twitch muscle fibers. By acting as a 'slow-onset' Ca^{2+} buffer, PV does not affect the rapid contraction phase, but significantly contributes to increase the rate of relaxation, as demonstrated in PV–/– mice. Unexpectedly, PV–/– fast-twitch muscles were considerably more resistant to fatigue than the wild-type fast-twitch muscles. This effect was attributed mainly to the increased fractional volume of mitochondria in PV–/– fast-twitch muscle, *extensor digitorum longus*, similar to levels observed in the slow-twitch muscle, *soleus*. Quantitative analysis of selected mitochondrial proteins, mitochondrial DNA-encoded cytochrome oxidase *c* subunit I and nuclear DNA-encoded cytochrome oxidase *c* subunit Vb and F1-ATPase subunit β revealed the PV–/– *tibialis anterior* mitochondria composition to be almost identical to that in wild-type *soleus*, but not in wild-type fast-twitch muscles. Northern and western blot analyses of the same proteins in different muscle types and in liver are indicative of a complex regulation, probably also at the post-transcriptional level. Besides the function in energy metabolism, mitochondria in both fast- and slow-twitch muscles act as temporary Ca^{2+} stores and are thus involved in the shaping of Ca^{2+} transients in these cells. Previously observed altered spatio-temporal aspects of Ca^{2+} transients in PV–/– muscles are sufficient to up-regulate mitochondria biogenesis through the probable involvement of both calcineurin- and Ca^{2+}/calmodulin-dependent kinase II-dependent pathways. We propose that 'slow-twitch type' mitochondria in PV–/– fast muscles are aimed to functionally replace the slow-onset buffer PV based on similar kinetic properties of Ca^{2+} removal.

Parvalbumin (PV) is a soluble calcium-binding protein that is highly expressed in fast-twitch muscle fibers [1] and specific neurons, including Purkinje cells and GABAergic interneurons [2]. Although its putative role acting as a temporary Ca^{2+} buffer is still under debate, there is growing evidence that PV is a key player in intracellular Ca^{2+} buffering [3,4]. In mammalian fast-twitch muscles, PV facilitates the rapid relaxation by acting as a temporary Ca^{2+} buffer [5]. Furthermore, PV–/– fast-twitch muscles were found to be significantly more resistant to fatigue than the wild-type fast-twitch muscles [6]. The fatigue resistance and ability to sustain muscle activity for prolonged periods of time is a principal functional hallmark of slow-twitch type I myofibers (which do not express PV and contain a high fractional volume of mitochondria) because they utilize oxidative metabolism

Abbreviations
AL, *adductor longus*; CaN, calcineurin; CaMKII, calmodulin-dependent kinase II; CLFS, chronic low-frequency stimulation; COX, cytochrome *c* oxidase; EDL, *extensor digitorum longus*; GAPDH, glyceraldehyde-3-phosphate dehydrogenase; MLC, myosin light chain; PV, parvalbumin; SERCA, sarcoendoplasmic reticulum Ca^{2+}-ATPase; SOL, *soleus*; TA, *tibialis anterior*; TnI_{fast}, troponin I fast; WT, wild type.

as their main source of energy. In contrast, muscles composed of fast-twitch type II fibers are susceptible to fatigue, in part because of their mainly glycolytic metabolism [7]. In compliance with the increased fatigue resistance of PV–/– fast-twitch muscles, the fractional volume of mitochondria in the fast-twitch muscle *extensor digitorum longus* (EDL) was almost doubled in PV–/– mice. Induction of muscle mitochondria biogenesis represents an important adaptation mechanism of all muscle types to increased demands of energy as a result of extensive work and chronic exercise [8]. The mechanism of control of mitochondrial biogenesis in muscles in response to muscle activity, as well as the mechanism controlling differential biogenesis of mitochondria associated with particular muscle fiber types, is not yet clear. The putative signals coupling muscle activity with the pathway of gene expression probably arise from combinations of accelerations in ATP turnover or imbalances between mitochondrial ATP synthesis and cellular ATP demand, and Ca^{2+} fluxes [8]. An increased biogenesis of mitochondria was detected in skeletal muscle of null-mutant mice for proteins involved in ATP metabolism, such as creatine kinase [9] and the ADP/ATP translocator [10]. Intracellular Ca^{2+} acts as an important second messenger controlling many cell functions and processes, including gene expression [11]. Increased biogenesis of mitochondria has been described as consequence of elevated intracellular Ca^{2+} levels [12]. Although the nuclear targets responsible for Ca^{2+}-induced expression of mitochondrial proteins are not well understood, studies of pathways downstream of contractile activity have implicated Ca^{2+} signaling through calcineurin (CaN) [13] and calmodulin kinase [14] to play an important role. In addition, a recent study indicates an involvement of Ca^{2+} signaling in the control of both mitochondrial biogenesis and fiber-type specific switch of gene expression [15].

As Ca^{2+} transients in PV–/– fast-twitch muscles were shown to be different from those of wild-type (WT) fast-twitch muscles [6], and because the mitochondrial volume was increased to levels found in slow-twitch fibers, a detailed study on mitochondrial proteins, fiber-type specific proteins and selected metabolic enzymes was carried out.

Results

No differences in fiber-type specific proteins between PV–/– and WT muscles

Previously reported alterations in the composition of increased resistance of muscle constituents and PV–/– fast-twitch muscle to fatigue [5,6,16] were in line with the conversion of a fast- to a slow-twitch muscle, and similar to the effects detected after chronic low-frequency stimulation (CLFS) of a fast-twitch muscle [17]. In contrast to CLFS, all muscle type specific components investigated so far, troponin T [5] and myosin heavy chain isoforms [16], were found to be of the fast-type in PV–/– fast-twitch muscles. In addition, the total activity of sarcoendoplasmic reticulum Ca^{2+}-ATPase (SERCA) was unchanged [16]. The increased mitochondrial volume in PV–/– EDL [6] prompted us to analyze, in detail, mitochondrial alterations and to investigate the presence of additional putative compensation mechanisms in PV–/– fast-twitch muscles. *Tibialis anterior* (TA) was selected, which contains a majority of fast-twitch PV-positive fibers and high

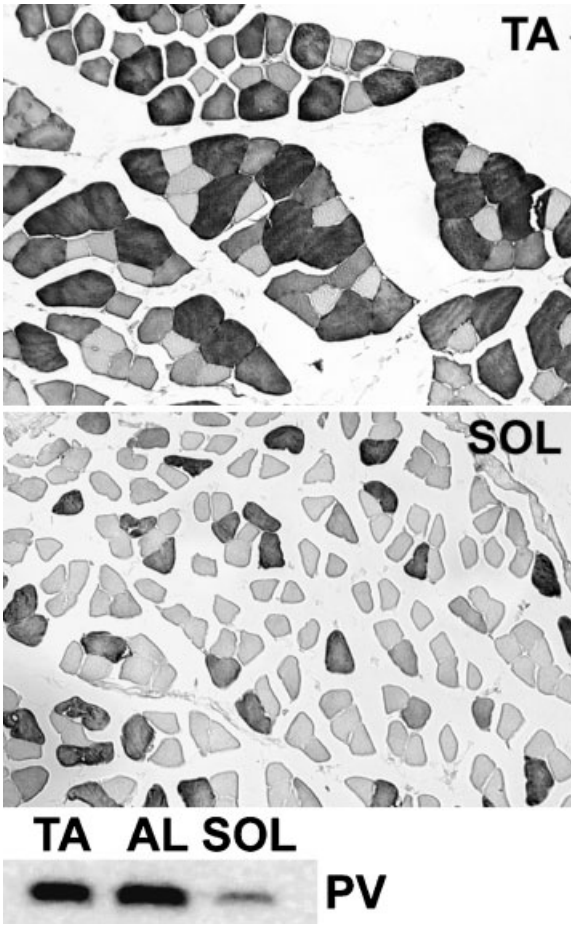

Fig. 1. Immunohistochemistry and western blot analysis for parvalbumin (PV) in *tibialis anterior* (TA), *adductor longus* (AL) and *soleus* (SOL) in an adult wild-type (WT) mouse. The percentage of PV-immunostained (dark) fibers is much higher in TA than in SOL. This is reflected by the stronger PV signal in the western blots (lower part) of protein extracts from the fast-twitch muscles, TA and AL, in comparison to the slow-twitch muscle, SOL.

protein levels of PV (Fig. 1). In a few experiments, *adductor longus* (AL) was used, another fast-twitch muscle containing slightly higher levels of type I slow-twitch fibers compared with TA [18] and comparable amounts of PV (Fig. 1). In addition, the slow-twitch muscle, *soleus* (SOL), mainly composed of slow PV-negative type I fibers, expressing significantly less PV (Fig. 1), was analyzed.

2D gel electrophoresis (Fig. 2) was carried out to compare protein expression patterns between PV–/– and WT TA. No significant differences in protein profiles were observed, with the exception of the missing spot corresponding to PV in PV–/– samples (Fig. 2). Several proteins were identified by comparison of 2D gels with a 2D gel of mouse *gastrocnemicus* muscle, available on the Expasy database (Table 1). The analysis was focused on the fiber-specific myosin light chain (MLC) isoform pattern and on two proteins implicated in muscle metabolism (creatine kinase and β-enolase). Significant differences between TA and SOL were evident (Fig. 2C,D). While fiber specific isoforms MLC1 and MLC2 are present both in TA and SOL, MLC3 is restricted to fast-twitch fibers, the weak signal in SOL probably the result of a small percentage of fast fibers in SOL. Although absolute levels of MLC3 and PV are much higher in TA than in SOL, the ratio of the two proteins in each of the two muscles seemed to be constant (Fig. 2C). A high degree of homology between short segments of putative promoter regions of the PV and MLC3F gene has been previously observed. A segment of 32 bp was identical in both genes and, based on these findings, the authors proposed that the expression of PV and MLC3F might be regulated in a similar way [19]. When comparing the MLC region of the 2D gels between TA from PV–/– and PV+/+ mice, the pattern is virtually identical with the exception of the lack of the PV spot in PV–/– mice (Fig. 2A–C). This indicates that expression of fiber type specific MLC isoforms is not affected by PV deficiency, in line with previous findings that a lack of PV does not change the myosin heavy chain pattern [16]. Also, two cytosolic enzymes – creatine kinase and β-enolase – involved in muscle metabolism are easily identified on 2D gels. While signals in TA from PV–/– and WT were of similar size (even slightly stronger in PV–/– TA), the signals in SOL were much weaker (Fig. 2D). Proteomic analysis of fiber specific proteins was complemented by western blot analysis and RT-PCR of troponin I fast (TnI_{fast}) isoform and SERCA2a, respectively. No changes in the protein expression levels of TnI_{fast} were observed in TA of either genotype (Fig. 3A). As SERCA2a, expressed in slow-twitch type I fibers [20], exhibits high plasticity after

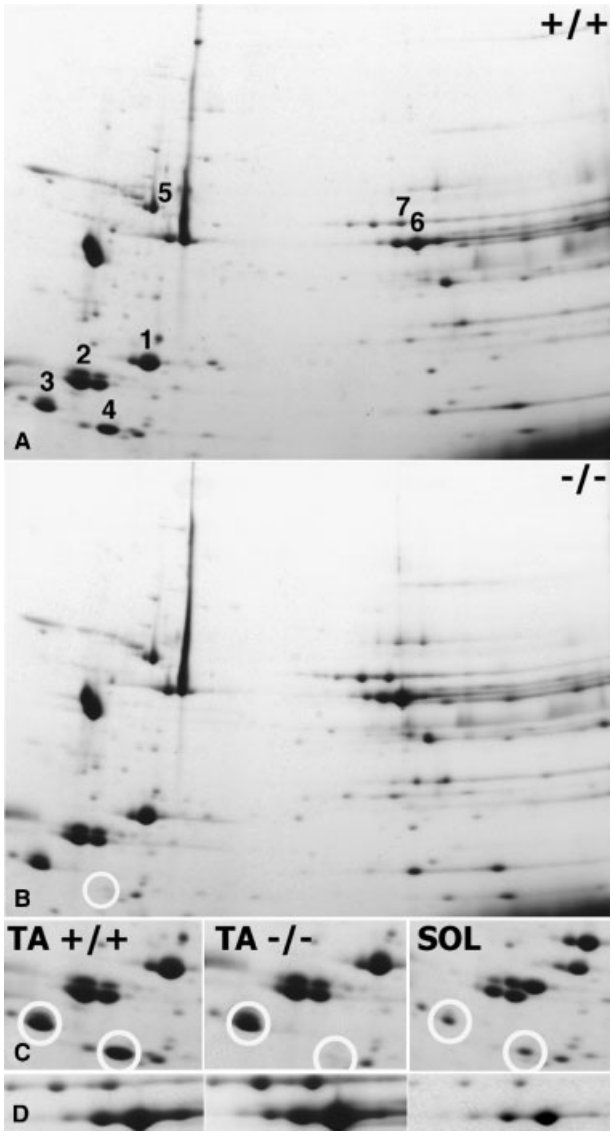

Fig. 2. 2D gel electrophoresis of protein extracts of *tibialis anterior* (TA) from (A) wild-type (WT) (+/+) and (B) parvalbumin (PV)–/– mice. Isoelectric focusing was carried out between pH 3 and 10, and the second dimension was run on a 9–16% gradient SDS polyacrylamide gel. Identified proteins are numbered from 1 to 7 and details are found in Table 1. The most striking difference is spot 4 (PV), which is missing on the gel of the PV–/– sample (circle). (C) The region (approximate range: molecular mass 10–25 kDa, pI 4.2–5.2) containing myosin light chain (MLC) isoforms 1, 2, 3, and PV, are shown for TA from WT (+/+) and PV–/– mice and from WT SOL. The main differences between TA and SOL are the significantly smaller spots 4 (PV) and 3 (MLC 3) in SOL. Both spots (MLC 3: left; PV: right) are marked by circles. (D) The region consisting of creatine kinase (spot 6; lower lanes) and β-enolase (spot 7, upper lanes) of the same samples as in (C) is shown. Signal intensities in PV–/– TA are as in WT TA, not as in WT SOL.

Table 1. Proteins identified on 2D gels by comparison with a web-based database. Protein spots were assigned by comparison with a 2D database of mouse *gastrocnemius* muscle (http://µsexpasy.org/cgi-bin/map2/def?MUSCLE_MOUSE). The standard 2D pattern was calibrated by the theoretical M_r/pI values of identified proteins. M_r/pI values listed in the Table were estimated from calibrated gels.

Spot no.	Protein identification	SWISS-PROT accession number	M_r (Da)	pI
1	Myosin light chain 1	P05977	18 941	5.07
2	Myosin light chain 2	P97457	16 642	4.66
3	Myosin light chain 3	P05978	14 310	4.48
4	Parvalbumin	P32848	12 305	4.84
5	F1-ATPase β-subunit	P19511	51 080	5.05
6	Creatine kinase, M chain	P07310	41 171	6.65
7	β-enolase	P21550	46 858	6.54

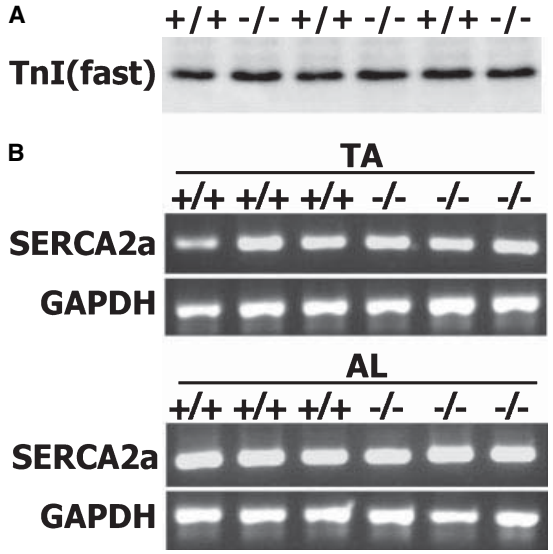

Fig. 3. (A) Western blot analysis of the fast isoform of troponin I (TnI_{fast}) in *tibialis anterior* (TA) of wild-type (WT) (+/+) and parvalbumin (PV)–/– ($n = 3$) mice. No differences were observed between the two genotypes. (B) RT-PCR for the slow-twitch muscle isoform sarcoendoplasmic reticulum Ca^{2+}-ATPase 2a (SERCA2a) in TA (upper panel) and in *adductor longus* (AL; lower panel). As a control for input RNA, glyceraldehyde-3-phosphate dehydrogenase (GAPDH) RT-PCR was used as a control. No significant differences between WT and parvalbumin (PV)–/– mice were observed ($n = 3$ animals for each genotype).

CLFS of a fast-twitch muscle [21], RT-PCR was carried out to detect putative changes of SERCA2a mRNA levels in the TA and AL of PV–/– mice. The optimal number of PCR cycles was found to be 27 for SERCA2a mRNA in TA and AL (data not shown), where differences in input mRNA were related directly to the amounts of PCR amplicon. The signal in AL was clearly stronger than in TA (Fig. 3B), which is in line with previous findings that (a) expression levels of SERCA2a are low in fast-twitch muscles [22] and (b) AL contains more slow-twitch fibers than TA [18]. As a control for input mRNA levels, RT-PCR for glyceraldehyde-3-phosphate dehydrogenase (GAPDH) was carried out. In neither TA nor AL were significant differences in SERCA2a levels detected between PV–/– and WT samples, further indicating that all fiber-type specific components of the contractile complex, and also endoplasmic reticulum proteins involved in Ca^{2+} homeostasis, are not affected by the absence of PV.

Mitochondrial proteins are affected differently by PV deficiency in fast-twitch muscles

Quantitative western blot analysis (Fig. 4A) revealed that the cytochrome *c* oxidase subunits I and Vb (COX I and COX Vb, encoded by mitochondrial and nuclear DNA, respectively), as well as cytochrome *c*, were significantly up-regulated in TA muscles of

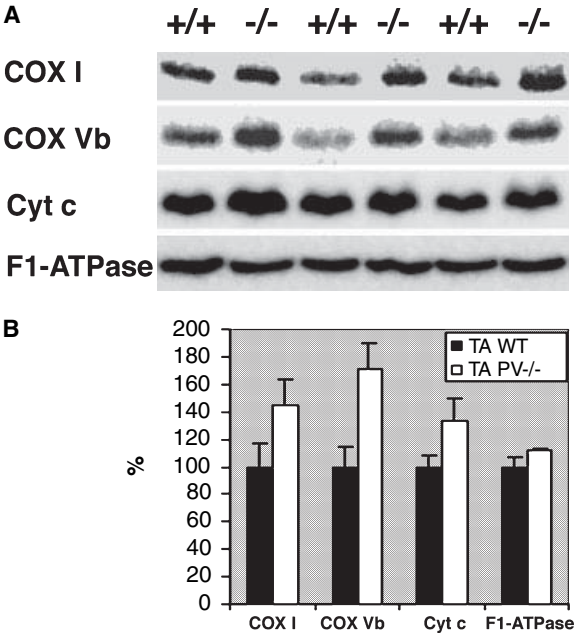

Fig. 4. Quantitative western blot analysis of the mitochondrial proteins cytochrome *c* oxidase subunits I and Vb (COX I and COX Vb, respectively), cytochrome *c* (Cyt *c*) and the beta subunit of the F1-ATPase isolated from *tibialis anterior* (TA). Mean protein levels of the four proteins in wild-type (WT) (+/+) mice were set to 100%. (A) Western blot signals (as determined using the ECL chemiluminescence method) from three individual mice from each genotype. Direct images were obtained from Phosphoimager. (B) Quantitative analysis of four to nine mice per genotype, and samples, were quantified from three independent western blot membranes. Values represent the mean ± SEM. *P*-values were calculated using the Student's *t*-test [WT vs. parvalbumin (PV)–/–] and are < 0.01 (COX I), < 0.001 (COX Vb), < 0.005 (Cyt *c*) and < 0.05 (F1-ATPase).

PV–/– mice (Fig. 4B). These results support the morphometric results of an increase in mitochondrial volume and indicate that the expression of several proteins, encoded by both the mitochondrial and the nuclear genome, is affected by a lack of PV. Interestingly, the increase in protein expression levels of F1-ATPase β between WT and PV–/– muscles (12%) was much less pronounced than for both COX isoforms (44% and 71% increase for COX I and COX Vb, respectively) and for cytochrome *c* (34%). Ca^{2+} signals play an important role in the regulation of gene expression in excitable tissue [11]. Increased transcription of the cytochrome *c* gene has been described after incubation of myotube cultures with the Ca^{2+} ionophore, A23187 [23]. In addition, increased transcription of mitochondrial genes has been observed as the result of permanent activation of some components of Ca^{2+} signaling pathways [13,14,24]. Based on this, we hypothesized that the prolongation of Ca^{2+} transients observed in PV–/– muscles might differentially affect Ca^{2+} signaling pathways, the best characterized in muscle being the CaN and the calmodulin-dependent kinase II (CaMKII) pathways. Quantitative RT-PCR revealed that the CaN signal was elevated: 132 ± 5% vs. 100 ± 8% (mean ± SEM; $P < 0.05$) for PV–/– and WT, respectively ($n = 4$ mice per genotype). In addition, CaN activity was doubled in extracts from PV–/– TA compared with WT: 212 ± 43% vs. 100 ± 27%, respectively (mean ± SEM; $P < 0.05$, $n = 9$ animals per genotype). Moreover, increases for CaMKII RT-PCR signals were detected [123 ± 11% vs. 100 ± 2% (mean ± SEM; $P < 0.05$) for PV–/– and WT, respectively; $n = 6$ and 7 animals, respectively]. We conjectured that the alteration in Ca^{2+} transients and Ca^{2+} signal transduction pathway observed in PV–/– muscles might be sufficient to induce the transcription of genes encoding mitochondrial proteins. To test this hypothesis, we determined the mRNA levels for COX I, COX Vb and F1-ATPase β. The levels of F1-ATPase β mRNA were not significantly different between the TA of WT and PV–/– (ratio PV–/– : WT = 0.95; not significant), in accordance with the almost unchanged protein levels described above. Although the protein levels of both COX I and COX Vb were increased in the TA of PV–/– mice, only insignificant increases in COX mRNA levels, in the order of 5%, were observed (Fig. 5). These observations are compatible with an altered post-transcriptional regulation of expression of COX I and Vb in PV–/– and WT TA. This raised the question of whether such a regulation was specific for PV–/– fast-twitch muscles, or if such differences in the regulation also existed in different muscle types.

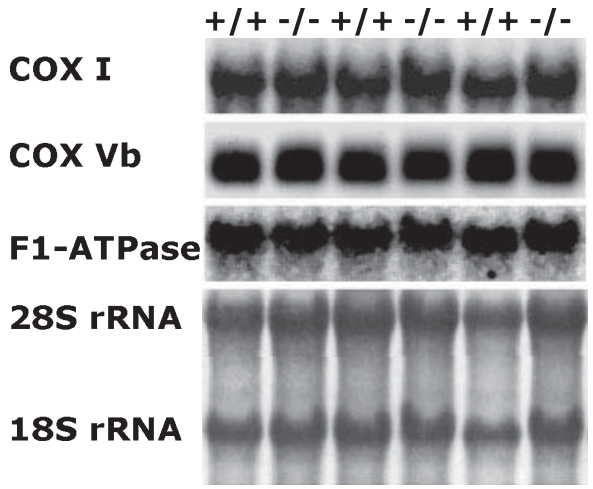

Fig. 5. Northern blot analysis of cytochrome *c* oxidase (COX) I, COX Vb and F1-ATPase from total RNA isolated from *tibialis anterior* (TA) of wild-type (WT) (+/+) and parvalbumin (PV)–/– mice. As a loading control, the methylene blue-stained membrane after RNA transfer is shown. No significant differences in the mRNA levels of all three genes were detected.

Mitochondrial protein levels are differently regulated in various muscle types and liver

The regulation of COX I, COX Vb and F1-ATPase β in different muscle types and in a nonmuscle tissue (liver) was investigated. Protein and mRNA levels of COX I, COX Vb and F1-ATPase β were quantified in TA, SOL, heart and liver. Western blot analysis revealed highly significant [two-way analysis of variance (ANOVA), all $P < 0.001$] differences in COX I, COX Vb and F1-ATPase β protein levels among fast-twitch, slow-twitch, heart muscle and liver (Fig. 6, Table 2). The highest levels of COX I and COX Vb were found in heart, followed by SOL, with TA having the lowest expression levels. This is directly correlated with the different amounts of mitochondria present in these muscles. On the other hand, COX I mRNA levels were almost identical in the three muscle types, although protein levels were increased by 35% and approximately fivefold in SOL and heart, respectively, when compared with TA. Very similar results were also found for COX Vb protein and mRNA levels, as well as for F1-ATPase β (TA, SOL and heart, Fig. 6 and Table 2). Yet another situation was observed in liver; mRNA levels of all three investigated proteins (Fig. 6) were significantly lower in liver (on average only ≈20% in comparison to TA), while protein levels were comparable to those found in TA (Fig. 6 and Table 2).

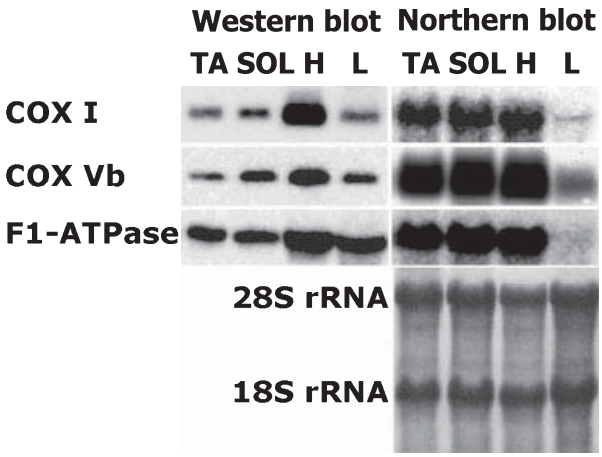

Fig. 6. Western blot and northern blot analysis of cytochrome *c* oxidase (COX) I, COX Vb and F1-ATPase of adult (2–4 months old) wild-type (WT) mice. Either total RNA or protein extracts from *tibialis anterior* (TA), *soleus* (SOL), heart (H) or liver (L) were analyzed. In the northern blot, the methylene blue-stained membrane after RNA transfer is shown. The striking differences in the ratio between mRNA and protein signals in the different tissues is indicative of complex regulation (see the Results and Discussion sections).

A final comparison between the mRNA and protein levels of COX I, COX Vb and F1-ATPase β, between SOL and TA on the one hand and between PV–/– and WT TA on the other, revealed striking similarities. There were almost no differences in the mRNA and protein levels of both COX isoforms between WT SOL and PV–/– TA. In both cases, COX Vb was up-regulated more (+53% and +71% in WT SOL and PV–/– TA, respectively) than COX I (+35% vs. +44%). The increase in protein levels of F1-ATPase β was much less pronounced (+13%; WT SOL vs. +11%; PV–/– TA), but was almost identical in the two samples. Thus, the biogenesis of mitochondria resulting from the absence of PV in fast-twitch PV–/– TA is not the result of a simple increase of all mitochondrial constituents. Based on the increased mitochondrial volume in PV–/– TA described previously (+85%) [6], the increase in surface is estimated to be in the order of 50%, conjecturing the mitochondrial shape to be ellipsoid. To substantiate whether this assumption also holds true for the inner mitochondrial membrane with its complex geometry, the cardiolipin content, a marker of the inner mitochondrial membrane, was established. An increase of ≈40% in PV–/– TA membranes was found when compared with WT (2.89 ± 0.21 vs. 2.06 ± 0.32 nmol cardiolipin per mg of total phospholipid phosphate, respectively; $P < 0.01$; $n = 4$ mice per genotype). An up-regulation of that order is found for both COX isoforms, as well as for cytochrome *c*. On the other hand, the up-regulation of F1-ATPase β was clearly smaller and comparable to the composition of SOL mitochondria, indicative of a regulated mechanism, as discussed below. In addition, the fact that protein levels of COX I and COX Vb, but not mRNA levels, are increased in SOL and PV–/– TA suggest that these differences are the result of translational, rather than transcriptional, control.

Table 2. Relative amounts of cytochrome *c* oxidase (COX) I, COX Vb and F1-ATPase subunit β protein and mRNA in *tibialis anterior* (TA), *soleus* (SOL), heart and liver. The concentrations of COX I, COX Vb and F1-ATPase subunit β were determined by quantitative western blot analysis using membrane protein fractions. Specific signals were evaluated by Phosphoimager analysis (Bio-Rad) and the relative concentration of each protein is expressed as a percentage relative to the mean value observed in TA. The mRNA concentration was determined by northern blot analysis using total RNA (20 μg of total RNA for each tissue); the TA signal was defined as 100%. The two values for the northern blots were obtained from two independent experiments. For muscle samples, tissue from three animals were pooled, thus the two values represent the mean of two × three mice. Western blot results are least-square means (corrected for missing values) +1 SE for a sample size of four to eight animals and from two or more independent experiments. SE values were calculated based on the residuals from the two-way analysis of variance (ANOVA). Capital letters indicate the results of the Waller-Duncan *k*-ratio test; mean values labeled with different letters are significantly different from each other ($P < 0.05$).

	Gene					
	COX I		COX Vb		F1-ATPase	
Tissue	Protein	mRNA	Protein	mRNA	Protein	mRNA
TA	100 + 5 C	100	100 + 10 B	100	100 + 8 B	100
SOL	135 + 13 B	102	153 + 31 B	113	113 + 4 B	134
		104		113		172
Heart	457 + 46 A	103	544 + 82 A	121	393 + 58 A	181
		104		127		133
Liver	111 + 4 C	20	141 + 8 B	18	146 + 22 B	14
		14		24		32

ATP content in fast-twitch muscle is affected by PV deficiency

Not only the volume and biochemical composition of mitochondria, but also the concentrations of ATP and phosphocreatine, are different between fast- and slow-twitch muscles [25]; ATP values are ≈60% higher in EDL than in SOL. Analyses of ATP levels in TA and SOL from WT yielded similar results: 2.52 ± 0.25 vs. 1.28 ± 0.26 μmol ATP·g^{-1} wet weight of muscle ($P < 0.02$) (i.e. an increase of almost twofold). While ATP levels in PV–/– SOL (1.31 ± 0.04) were indistinguishable from those of WT SOL, the ATP levels in PV–/– TA (1.57 ± 0.29) were clearly lower than in WT TA ($P < 0.05$), yet not statistically different from those in either WT or PV–/– SOL.

Discussion

Skeletal muscle fibers display a large degree of plasticity [7,26], including rearrangement of gene expression of myofibrillar and other protein isoforms (such as mitochondrial proteins), and may result in fiber type transitions. This process occurs in a sequential order and has been shown to be regulated by the EF-hand Ca^{2+} binding protein calmodulin, via CaN-dependent, calmodulin-dependent protein phosphatase [13,27–29] and CaMK pathways [14]. Evidence has accumulated that the transcription of fiber specific proteins and mitochondrial proteins is regulated by two distinct pathways, although both processes are initiated by Ca^{2+} signals [14]. In contrast to CLSF, where changes in fiber type specific proteins and mitochondrial proteins are observed, the lack of PV in the fast-twitch muscles of PV–/– only induced the latter process [6] and here we show that also MLC isoforms are not changed in PV–/– TA. Unaltered mRNA levels of TnI_{fast} and the slow isoform, SERCA2a, together with previous results [5,6,16], clearly demonstrate that signaling pathways linked to fiber specific isoforms are not activated in PV–/– fast-twitch muscles. Additionally, the investigated enzymes involved in muscle metabolism, creatine kinase and β-enolase were found, in PV–/– TA, to be expressed at levels found in WT TA and not at much lower levels, as seen in SOL. These findings further support the presence of distinct pathways regulating fiber specific isoforms and metabolic enzymes, on the one hand, and mitochondrial biogenesis, on the other.

Renewed interest in mitochondria was brought about by the recognition of their role in apoptosis [30], Ca^{2+} homeostasis [31] and signal transduction [32]. In skeletal muscles, mitochondria provide most of the energy under aerobic conditions and display relatively high plasticity [8,33]. Significant variations in the oxidative capacity of different muscles exist in order to meet their physiological demands. Heart muscle exhibits the highest content of mitochondria, as well as the largest oxidative capacity, as a result of the permanent workload. Slow-twitch muscles involved in posture and endurance performance contain significantly fewer mitochondria than heart muscle, but still more than fast-twitch muscles that are optimized for short, rapid movements. In addition to muscle-specific differences in mitochondrial volume, the oxidative capacity of muscles is also affected by physiological conditions, such as chronic exercise or contraction activity. Increased oxidative capacity of muscles is normally associated with an increase of mitochondrial density, and mitochondrial biogenesis has been observed after chronic exercise and CLFS of fast-twitch muscle [34].

Mitochondrial biogenesis requires the coordinated expression of gene products encoded by mitochondrial DNA and nuclear DNA, with the appropriate stochiometry of all mitochondrial proteins [33]. Based on the twofold increase in mitochondrial volume in PV–/– fast-twitch muscles [6] we addressed the question of whether the profile of selected mitochondrial proteins corresponds to the one observed in either fast- or slow-twitch muscles. Beforehand, we evaluated whether such differences at the level of mRNA or protein existed between mitochondria from fast-twitch (TA) or slow-twitch (SOL) muscles and in two other tissues – heart muscle and liver. Significant differences in protein and/or mRNA levels of COX I, COX Vb and F1-ATPase β in the four tissues – TA, SOL, heart and liver – are indicative of a complex regulation, probably involving post-transcriptional regulation.

Evidently, mRNA and protein levels of the above proteins in PV–/– TA were of major interest: mRNA levels of both COX species were identical as in WT SOL and TA, while protein expression levels were practically identical to those in WT SOL (i.e. significantly higher than in WT TA). Thus, PV deficiency induces regulated mitochondrial biogenesis of 'slow-twitch' mitochondria in TA, resulting in a mitochondrial volume and a biochemical composition as found in slow-twitch muscle. Also with respect to ATP content in a resting muscle, which is apparently regulated by the muscle-type specific mitochondria, TA from PV–/– has properties like a slow-twitch muscle. Mitochondria in different tissues are tailored to meet both metabolic and signaling needs with respect to the expression levels of individual mitochondrial proteins. By proteomics, significant differences in the abundance of mitochondrial proteins in mitochondria from brain, heart, kidney and liver were observed [35]. Our results

indicate that the same holds true for fast- and slow-twitch muscles.

Recently, mitochondria have regained much interest as temporary Ca^{2+} stores, as opposed to the classical role in energy metabolism [36], also in muscles. A significant contribution of mitochondria in the muscle relaxation of fast-twitch muscles, [37] and even more importantly in slow-twitch muscles [38,39], has been demonstrated. During a single twitch in TA recorded *in vivo*, mitochondria take up Ca^{2+} with a delay of $\approx$20 ms as compared to rises in $[Ca^{2+}]_i$, and peak $[Ca^{2+}]_m$ was reached during the relaxation phase. Thus, the effect of mitochondria on $[Ca^{2+}]_i$ is very similar to the role of PV (i.e. to promote an increase in the initial rate of $[Ca^{2+}]_i$ decay). The up-regulation of mitochondria in PV–/– TA might thus be viewed as a homeostatic compensation mechanism with kinetically similar characteristics as PV. Indirect functional evidence for mitochondria contributing to Ca^{2+} removal in PV–/– TA has been presented previously [6]. Besides the predicted slowing of the initial $[Ca^{2+}]_i$ decay phase in PV–/– TA, the kinetics of Ca^{2+} transients at later time-points (200–700 ms) were altered. Differences were not in the expected direction (i.e. a slower decay at later time-points) [40,41], but after 200 ms, $[Ca^{2+}]_i$ was even lower than before the stimulation, resulting in negative $\Delta[Ca^{2+}]$ values, of −40 nM, in PV–/– fast-twitch muscle flexor digitorum brevis [6]. As the activity of the sarcoplasmic reticulum Ca^{2+}-ATPase was not different between WT and PV–/– samples, the most probable candidate contributing to enhanced Ca^{2+} clearance in PV–/– fast-twitch muscles was hypothesized to be mitochondria.

Is there further evidence that different types of mitochondria are specifically well suited as transient Ca^{2+} sinks? Results of the mitochondrial F1-ATPase β levels hint in this direction. A regulation of this protein at the translational level in adult liver has been documented by *in vitro* translation experiments [42]. Compared with protein increases in the order of 50% in COX I and Vb levels in WT SOL and PV–/– TA, increases in F1-ATPase β were only $\approx$10%. Assuming that translational regulation is both protein- and tissue-type dependent, it can adapt the respiratory chain to physiological demands. For example, F1-ATPase protein levels are strongly reduced in brown fat tissue as a consequence of translational regulation [43], leading, together with uncoupler protein (UCP) expression, to increased heat production. As discussed before, besides ATP production, transient Ca^{2+} uptake in excitable cells (fast-twitch muscle [37], neurons [44]) is an additional important function of mitochondria. Rapid Ca^{2+} uptake occurs via a putative uniporter [45] driven by the proton gradient established across the inner mitochondrial membrane by means of a proton translocating system including the COX complex [31]. Thus, an increased level of COX, and an almost constant level of F1-ATPase observed in WT SOL and PV–/– TA, increases the oxidative capacity, which in turn might lead to a more robust Ca^{2+} uptake by these mitochondria, as the uniporter can transport Ca^{2+} ions, as long as the mitochondrial membrane potential is maintained. Nonetheless, the additional mitochondria in PV–/– TA do not exactly match, with respect to the kinetics of Ca^{2+} uptake, to the situation present in WT TA, as both $[Ca^{2+}]_i$ decay and relaxation were still slower in PV–/– than in WT fast-twitch muscle [6].

How could PV, a soluble cytoplasmic protein, affect the expression of mitochondrially encoded proteins? The most obvious explanation is that subtle alterations, in the shape of Ca^{2+} transients, are sufficient to regulate mitochondrial biogenesis via Ca^{2+}-dependent pathways, probably involving CaMKII and CaN-dependent pathways, in accordance with our RT-PCR results of increased PCR signals in PV–/– TA. The twofold increase also observed in CaN activity supports a prominent role for the CaN-mediated pathway in this process. Two lines of evidence indicate that the inverse regulation of PV and mitochondrial volume is a universal one, namely (a) ectopic expression of PV in the slow-twitch muscle SOL led to a decrease in succinate dehydrogenase activity [46] possibly a result of decreased mitochondria, and (b) the mitochondrial volume of striatal neurons ectopically expressing PV was reduced to almost half of the volume measured in WT neurons [47]. The exact signal(s) influenced by the lack of PV, which is transmitted to mitochondria affecting mitochondrial translation, is currently unknown. This is not specific for the situation in PV–/– cells, but is also generally a still open question. In addition, our results indicate that translation and other post-transcriptional processes play an important role in the control of muscle fiber type differences, and in mitochondrial biogenesis in adult muscle.

Experimental procedures

Animals

PV-deficient mice were generated by homologous recombination, as described previously [5]. Adult (3–6 months old) male mice of both genotypes (WT and PV–/–) were used in this study. Appropriate measures were taken to minimize pain and discomfort of the animals used in this study. All experiments were performed in accordance to the European

Committee Council Directive of November 24, 1986 (86/609/EEC) and the Veterinary Office of Fribourg. Mice were deeply anesthetized by the inhalation of carbon dioxide and briefly perfused transcardially by ice-cold NaCl/P_i (PBS). The muscles TA, AL and SOL, as well as heart and liver, were immediately dissected, frozen in liquid nitrogen and stored at −70 °C until required for analysis. Tissue used for RNA isolation was dissected from mice perfused with sterile ice-cold NaCl/P_i prepared with diethyl pyrocarbonate-treated water. Muscles intended for immunohistochemistry were dissected from mice perfused first with NaCl/P_i and then with 4% paraformaldehyde. Dissected muscles were fixed additionally by immersion in 4% paraformaldehyde for 24 h and then washed in NaCl/Tris (TBS).

Quantitative western blot analysis

Unless stated otherwise, chemicals were obtained from Sigma-Aldrich (Buchs, Switzerland). Membrane protein fractions were prepared by homogenization of tissue in homogenization buffer [10 mM Tris/HCl, 1 mM EDTA, pH 7.4, and one tablet of protease inhibitor cocktail (Roche, Rotkreuz, Switzerland) added per 10 mL of buffer, just prior to use] using a Polytron homogenizer. Cell membranes were sedimented by centrifugation at 30 000 ***g*** for 30 min, resuspended in homogenization buffer and once more sedimented by centrifugation at 30 000 ***g*** for 30 min. Membrane pellets were resuspended in 1% SDS and membrane proteins were solubilized by the addition of 10% SDS to a final concentration of 5.5%. Total tissue extracts were prepared by homogenization of muscles in RIPA buffer [1 × NaCl/P_i, 1% (v/v) Nonidet P-40, 0.5% (w/v) sodium deoxycholate, 0.1% (w/v) SDS and one tablet of protease inhibitor cocktail (Roche) added per 10 mL of buffer just prior to use). Protein concentration was determined by the protein Dc assay kit (Bio-Rad, Glattbrugg, Switzerland). Membrane protein fractions (in the case of COX I, COX Vb and F1-ATPase) and total muscle extracts (in the case of TnI_{fast} and cytochrome *c*) were used for quantification. Proteins (25 μg) were separated by SDS/PAGE, then transferred onto nitrocellulose membranes by using a semidry transfer protocol. The membranes were controlled for even load and possible transfer artifacts by staining with Ponceau Red solution. After blocking with a 10% (w/v) solution of nonfat milk in NaCl/Tris containing 0.05% (v/v) Tween 20 (TBS-T buffer), membranes were incubated with primary antibodies against either COX I (1D6; 1 $\mu g \cdot mL^{-1}$; Molecular Probes, Leiden, the Netherlands), COX Vb (6E9; 2 $\mu g \cdot mL^{-1}$; Molecular Probes), F1-ATPase β (3D5; 0.2 $\mu g \cdot mL^{-1}$; Molecular Probes), cytochrome *c* (7H8.2C12; 1 $\mu g \cdot mL^{-1}$; BD PharMingen, Basel, Switzerland), fast troponin I (sc-8120; 1 : 1000 dilution; Santa Cruz Biotechnology, Santa Cruz, CA, USA) or PV (PV-4064; 1 : 3000 dilution; Swant, Bellinzona, Switzerland) for 90 min. All antibodies used were dissolved in TBS-T containing 1% (w/v) protease-free BSA. Incubation of membranes with primary antibodies was followed by extensive washing using TBS-T and consequently by the incubation of membranes with appropriate secondary biotinylated antibodies (1 : 10 000 dilution; Vector Laboratories, Burlingame, CA, USA). After extensive washing, membranes were incubated with avidin-biotin conjugated peroxidase (Vector Laboratories) solution in TBS-T and washed again. The bands corresponding to particular proteins were visualized and quantified by the Molecular Imager (Bio-Rad) using the ECL chemiluminescence method (Pierce, Perbio Science, Lausanne, Switzerland).

2D gel electrophoresis

2D gel electrophoresis was performed according to Langen *et al*. [48] with modifications. Samples were prepared by homogenization of muscles in 2D sample buffer [7 M urea, 2 M thiourea, 4% (w/v) CHAPS, 1% (w/v) dithioerythritol, 20 mM Tris, 0.02 (w/v) Bromophenol blue, 1 mM EDTA, one tablet of protease inhibitor cocktail (Roche) per 10 mL of sample buffer added just prior to use]. Protein concentration was determined by the Bradford assay (Bio-Rad). Proteins (0.75 mg) were first separated by isoelectric focusing on Immobiline Drystrips (Pharmacia, Amersham Biosciences Europe GmbH, Switzerland) with an immobilized linear pH gradient of 3 to 10. The next step comprised separation on a linear gradient of a 9–16% polyacrylamide gel. The gels were stained by Coomassie Blue R−250.

RNA isolation and RT-PCR

Total RNA was isolated using the guanidinium isothiocyanate method, according to Chomczynski & Sacchi [49]. Total RNA (1 μg) was reverse transcribed using the first-strand cDNA synthesis kit for RT-PCR (Roche). cDNA, corresponding to 0.2 μg of initial total RNA, was used in PCR reactions. Sequences of primers used for amplification of particular mRNAs are listed in Table 3. cDNA was amplified in standard PCR reaction buffer (Finnzymes, Bio-Concept, Allschwil, Switzerland) containing 0.2 mM each dNTP, 0.6 μM of each specific primer and 1 IU of *Taq* polymerase (Finnzymes). After initial denaturation at 94 °C for 3 min, cDNA was amplified using the optimal number of PCR cycles (midpoint of the logarithmic range). This was 27 cycles (in the case of SERCA 2a), 28 cycles (CaN), 35 cycles (CaMKII) or 25 cycles (GAPDH), consisting of denaturation at 94 °C for 20 s, annealing at 60 °C (SERCA 2a, GAPDH), 58 °C (CaN) or 55 °C (CaMKII) for 40 s, and an elongation step at 72 °C for 40 s. The final elongation step was carried out at 72 °C for 10 min. The PCR products were analyzed by electrophoresis on 2% agarose gels, and the ethidium bromide-stained bands were compared with marker bands of known sizes. Estimated sizes of amplified fragments were compared with the expected sizes

Table 3. Sequences of primers used for RT-PCR and synthesis of digoxigenin (DIG)-labeled DNA probes for northern blots. CaN, calcineurin; CaMKII, calmodulin-dependent kinase II; COX I, cytochrome *c* oxidase subunit I; COX Vb, cytochrome *c* oxidase subunit Vb; GAPDH, glyceraldehyde-3-phosphate dehydrogenase; SERCA2a, sarcoendoplasmic reticulum Ca^{2+}-ATPase 2a.

Name	Forward primer	Reverse primer	Amplicon size (bp)	Detection method
SERCA2a	GGC TCC ATC TGC TTG TCC ATG	GAA GCG GTT ACT CCA GTA TTG	204	RT-PCR
GAPDH	GAG CTG AAC GGG AAG CTC ACT GG	GTG AGG GAG ATG CTC AGT GTT GG	429	RT-PCR
CaN	AGTAACAATTTTCAGTGCTCCAAAC	AATATACGGTTCATGGCAATACTGT	205	RT-PCR
CaMKII	CTACCCCGGCGCTGGAGTCAAC	TCAGATGTTTTGCCACAAAGAGGTGCCTCCT	530	RT-PCR
COX I	CGA GCT TGC TTT ACA TCA GCC	TGT GTC ATC TAG GGT GAA GCC	317	Northern blot
COX Vb	GGC TTC AAG GTT ACT TCG CGG	TGG GGC ACC AGC TTG TAA TGG	371	Northern blot
F1-ATPase β	GGC GAA TCG TGG CAG TCA TCG	ACC ACC ATG GGC TTT GGC GAC	506	Northern blot

calculated from the gene bank databases. For quantitative RT-PCR analyses, images of CaN, CaMKII and GAPDH amplicons from the same sample were acquired with a charge-coupled device (CCD) camera and analyzed quantitatively using the Gene Tools (Syngene, Cambridge, UK) software. For each sample, the CaN/GAPDH and CaMKII/GAPDH ratios were calculated and the mean value of the WT group was set at 100%.

Northern blot analysis

RNA was separated by denaturing electrophoresis on formaldehyde-containing 1% agarose gels, then transferred onto positively charged nylon membranes (Roche) using the capillary downstream method. Membranes were controlled for even load and possible transfer artifacts by staining with methylene blue solution. The positions of 18S and 28S rRNA were marked on the membranes in order to estimate molecular sizes of particular signals. Membranes were prehybridized in ExpressHyb solution (Clontech, Basel, Switzerland) for 30 min at 58 °C and then hybridized with digoxigenin (DIG)-labeled cDNA probes for 60 min at 58 °C. All probes used in the study were synthesized by amplification of muscle cDNA using the kit for DIG-labeling of PCR probes (Roche) applying the manufacturer's protocol. Sequences of all primers are listed in Table 3. After hybridization, membranes were first washed twice with 0.1% (w/v) SDS in 1 × NaCl/Cit for 15 min at room temperature. The next step comprised a washing step with 0.1% (w/v) SDS in 0.1 × NaCl/Cit for 15 min at 55 °C. After washing, membranes were rinsed briefly in maleic acid buffer (0.1 M maleic acid, 0.15 M NaCl, pH 7.5) and then blocked in 1% (v/v) blocking reagent (Roche) solution in maleic acid buffer for 30 min at room temperature. Membranes were then incubated with anti-DIG immunoglobulin conjugated to alkaline phosphatase (1 : 4000 dilution; Roche) for 30 min. Membranes were washed twice with 3% (v/v) Tween-20 solution in maleic acid buffer for 15 min and then preincubated in detecting buffer (0.1 M Tris/HCl, 0.1 M NaCl, pH 9.5) for 5 min. Finally, membranes were incubated in detecting buffer containing CDP-star substrate (1 : 100; Roche). The bands corresponding to particular mRNAs were visualized and quantified by the Molecular Imager using the chemoluminescence screen (Bio-Rad).

Immunohistochemistry

Muscles were embedded in paraffin, cut to 5 μm sections and mounted on microscope glass supports. After deparaffinization, slices were rehydrated in NaCl/Tris and incubated with polyclonal anti-PV (PV-4064; 1 : 3000 dilution; Swant) for 24 h at 4 °C. After washing with TBS, sections were incubated with goat anti-rabbit biotinylated immunoglobulin (Vector) overnight at 4 °C. Secondary antibodies were removed by washing with NaCl/Tris and incubated with avidin-biotin conjugated peroxidase (Vector) for 2 h at room temperature. After extensive washing with NaCl/Tris, PV-positive fibers were visualized by incubation of sections with 3,3′-diaminobenzidine (DAB) and analysis of immunostained sections.

Cardiolipin measurements

Total lipids were extracted from TA membranes, as previously reported by Bligh & Dyer [50]. The extracted phoshopholipids were separated by 2D high-performance thin layer chromatography (HPTLC) on silica gel HPTLC plates (Merck). The position of cardiolipin on the plates was identified by chromatography of a cardiolipin standard (Sigma-Aldrich). Spots corresponding to cardiolipin were quantified by analysis of phospholipid phosphorus, as previously described by Rouser *et al*. [51]. The results are expressed as nmol of cardiolipin per mg of total phospholipid phosphate.

CaN activity assay

CaN activity was measured using the Calcineurin Cellular Activity Assay Kit (Calbiochem, VWR International AG, CH-6004 Luzern, Switzerland). Briefly, mice were perfused with NaCl/Tris, and bilateral TA muscle was excised and rinsed in NaCl/Tris. After homogenization in

the supplied lysis buffer, extracts were centrifuged at 45 000 ***g***, free phosphate was removed from the supernatant using P_iBind resin (Innova Biosciences, Babraham Hall, Barbraham, Cambridge, UK) and CaN activity was measured according to the manufacturer's instructions. Total CaN activity is expressed as a percentage vs. control animals and is normalized to soluble protein concentration, measured using the Dc assay (Pierce).

ATP measurements is isolated muscle

Bilateral TA and SOL muscles from NaCl/P_i-perfused mice ($n = 4$ mice per genotype) were homogenized in 2.5% (w/v) trichloroacetic acid, centrifuged (10 000 ***g***, 4 °C, 10 min) and the resulting supernatant was neutralized using 1 M Tris base (120 μL per 1 mL of supernatant). ATP measurements were carried out using the ATP Bioluminescence Assay Kit CLS II (Roche), according to the manufacturer's instructions. ATP concentrations are expressed as μmol of ATP·g^{-1} wet weight of muscle.

Statistical analysis

Western blot analyses were carried out using SAS version 8.2 (52). For the comparison of protein levels in different tissues, a two-way ANOVA test on log-transformed western blot data was performed. Additionally, the Waller-Duncan *k*-ratio test was carried out to test for pairwise differences in protein levels between tissues. For simple comparison of two groups (WT vs. PV–/–), the Student's *t*-test was used. Significance levels were set at $P < 0.05$.

Acknowledgements

The project was supported by the Swiss National Science Foundation (grants 3100–063448.00/1 and 3100A0-100400/1 to BS). We would like to thank S. Eichenberger for taking care of the animal facilities, Dr H. Langen, Roche, Basel for the introductory help with 2D gel electrophoresis and Dr T. Kawecki, University of Fribourg for the help in the statistical analyses.

References

1 Celio MR & Heizmann CW (1982) Calcium-binding protein parvalbumin is associated with fast contracting muscle fibres. *Nature* **297**, 504–506.
2 Celio MR (1990) Calbindin D-28k and parvalbumin in the rat nervous system. *Neuroscience* **35**, 375–475.
3 Schwaller B, Meyer M & Schiffmann SN (2002) 'New' functions for 'old' proteins: The role of the calcium-binding proteins calbindin D-28k, calretinin and parvalbumin, in cerebellar physiology. Studies with knockout mice. *Cerebellum* **1**, 241–258.
4 Gailly P (2002) New aspects of calcium signaling in skeletal muscle cells: implications in Duchenne muscular dystrophy. *Biochim Biophys Acta* **1600**, 38–44.
5 Schwaller B, Dick J, Dhoot G, Carroll S, Vrbova G, Nicotera P, Pette D, Wyss A, Bluethmann H, Hunziker W, *et al.* (1999) Prolonged contraction-relaxation cycle of fast-twitch muscles in parvalbumin knockout mice. *Am J Physiol* **276**, C395–C403.
6 Chen G, Carroll S, Racay P, Dick J, Pette D, Traub I, Vrbova G, Eggli P, Celio M & Schwaller B (2001) Deficiency in parvalbumin increases fatigue resistance in fast-twitch muscle and upregulates mitochondria. *Am J Physiol (Cell Physiol)* **281**, C114–C122.
7 Berchtold MW, Brinkmeier H & Muntener M (2000) Calcium ion in skeletal muscle: its crucial role for muscle function, plasticity, and disease. *Physiol Rev* **80**, 1215–1265.
8 Hood DA (2001) Invited Review: contractile activity-induced mitochondrial biogenesis in skeletal muscle. *J Appl Physiol* **90**, 1137–1157.
9 Veksler VI, Kuznetsov AV, Anflous K, Mateo P, van Deursen J, Wieringa B & Ventura-Clapier R (1995) Muscle creatine kinase-deficient mice. II. Cardiac and skeletal muscles exhibit tissue-specific adaptation of the mitochondrial function. *J Biol Chem* **270**, 19921–19929.
10 Murdock DG, Boone BE, Esposito LA & Wallace DC (1999) Up-regulation of nuclear and mitochondrial genes in the skeletal muscle of mice lacking the heart/muscle isoform of the adenine nucleotide translocator. *J Biol Chem* **274**, 14429–14433.
11 Carafoli E (2002) Calcium signaling: a tale for all seasons. *Proc Natl Acad Sci USA* **99**, 1115–1122.
12 Ojuka EO, Jones TE, Han DH, Chen M, Wamhoff BR, Sturek M & Holloszy JO (2002) Intermittent increases in cytosolic Ca^{2+} stimulate mitochondrial biogenesis in muscle cells. *Am J Physiol Endocrinol Metab* **283**, E1040–E1045.
13 Bigard X, Sanchez H, Zoll J, Mateo P, Rousseau V, Veksler V & Ventura-Clapier R (2000) Calcineurin co-regulates contractile and metabolic components of slow muscle phenotype. *J Biol Chem* **275**, 19653–19660.
14 Wu H, Kanatous SB, Thurmond FA, Gallardo T, Isotani E, Bassel-Duby R & Williams RS (2002) Regulation of mitochondrial biogenesis in skeletal muscle by CaMK. *Science* **296**, 349–352.
15 Lin J, Wu H, Tarr PT, Zhang CY, Wu Z, Boss O, Michael LF, Puigserver P, Isotani E, Olson EN, *et al.* (2002) Transcriptional co-activator PGC-1 alpha drives the formation of slow-twitch muscle fibres. *Nature* **418**, 797–801.
16 Raymackers JM, Gailly P, Schoor MC, Pette D, Schwaller B, Hunziker W, Celio MR & Gillis JM (2000) Tetanus relaxation of fast skeletal muscles of the mouse made parvalbumin deficient by gene inactivation. *J Physiol* **527**, 355–364.

17 Pette D & Vrbova G (1999) What does chronic electrical stimulation teach us about muscle plasticity? *Muscle Nerve* **22**, 666–677.
18 Seward DJ, Haney JC, Rudnicki MA & Swoap SJ (2001) bHLH transcription factor MyoD affects myosin heavy chain expression pattern in a muscle-specific fashion. *Am J Physiol Cell Physiol* **280**, C408–C413.
19 Berchtold MW (1989) Parvalbumin genes from human and rat are identical in intron/exon organization and contain highly homologous regulatory elements and coding sequences. *J Mol Biol* **210**, 417–427.
20 Quiroz-Rothe E & Rivero JL (2001) Co-ordinated expression of contractile and non-contractile features of control equine muscle fibre types characterised by immunostaining of myosin heavy chains. *Histochem Cell Biol* **116**, 299–312.
21 Hu P, Yin C, Zhang KM, Wright LD, Nixon TE, Wechsler AS, Spratt JA & Briggs FN (1995) Transcriptional regulation of phospholamban gene and translational regulation of SERCA2 gene produces coordinate expression of these two sarcoplasmic reticulum proteins during skeletal muscle phenotype switching. *J Biol Chem* **270**, 11619–11622.
22 Wu KD, Lee WS, Wey J, Bungard D & Lytton J (1995) Localization and quantification of endoplasmic reticulum Ca(2+)-ATPase isoform transcripts. *Am J Physiol* **269**, C775–C784.
23 Freyssenet D, Di Carlo M & Hood DA (1999) Calcium-dependent regulation of cytochrome c gene expression in skeletal muscle cells. Identification of a protein kinase c-dependent pathway. *J Biol Chem* **274**, 9305–9311.
24 Sayen MR, Gustafsson AB, Sussman MA, Molkentin JD & Gottlieb RA (2003) Calcineurin transgenic mice have mitochondrial dysfunction and elevated superoxide production. *Am J Physiol Cell Physiol* **284**, C562–570. Epub 2002 October 2023.
25 Kushmerick MJ, Moerland TS & Wiseman RW (1992) Mammalian skeletal muscle fibers distinguished by contents of phosphocreatine, ATP, and Pi. *Proc Natl Acad Sci USA* **89**, 7521–7525.
26 Pette D (2002) The adaptive potential of skeletal muscle fibers. *Can J Appl Physiol* **27**, 423–448.
27 Naya FJ, Mercer B, Shelton J, Richardson JA, Williams RS & Olson EN (2000) Stimulation of slow skeletal muscle fiber gene expression by calcineurin in vivo. *J Biol Chem* **275**, 4545–4548.
28 Di Liegro CM, Bellafiore M, Izquierdo JM, Rantanen A & Cuezva JM (2000) 3′-untranslated regions of oxidative phosphorylation mRNAs function in vivo as enhancers of translation. *Biochem J* **352**, 109–115.
29 Allen DL, Sartorius CA, Sycuro LK & Leinwand LA (2001) Different pathways regulate expression of the skeletal myosin heavy chain genes. *J Biol Chem* **276**, 43524–43533.
30 Hengartner MO (2000) The biochemistry of apoptosis. *Nature* **407**, 770–776.
31 Babcock DF, Herrington J, Goodwin PC, Park YB & Hille B (1997) Mitochondrial participation in the intracellular Ca^{2+} network. *J Cell Biol* **136**, 833–844.
32 Ichas F, Jouaville LS & Mazat JP (1997) Mitochondria are excitable organelles capable of generating and conveying electrical and calcium signals. *Cell* **89**, 1145–1153.
33 Moyes CD, Battersby BJ & Leary SC (1998) Regulation of muscle mitochondrial design. *J Exp Biol* **201**, 299–307.
34 Skorjanc D, Jaschinski F, Heine G & Pette D (1998) Sequential increases in capillarization and mitochondrial enzymes in low-frequency-stimulated rabbit muscle. *Am J Physiol* **274**, C810–C818.
35 Mootha VK, Bunkenborg J, Olsen JV, Hjerrild M, Wisniewski JR, Stahl E, Bolouri MS, Ray HN, Sihag S, Kamal M, *et al*. (2003) Integrated analysis of protein composition, tissue diversity, and gene regulation in mouse mitochondria. *Cell* **115**, 629–640.
36 Pozzan T & Rizzuto R (2000) High tide of calcium in mitochondria. *Nat Cell Biol* **2**, E25–E27.
37 Rudolf R, Mongillo M, Magalhaes PJ & Pozzan T (2004) In vivo monitoring of Ca(2+) uptake into mitochondria of mouse skeletal muscle during contraction. *J Cell Biol* **166**, 527–536.
38 Sembrowich WL, Quintinskie JJ & Li G (1985) Calcium uptake in mitochondria from different skeletal muscle types. *J Appl Physiol* **59**, 137–141.
39 Gillis JM (1997) Inhibition of mitochondrial calcium uptake slows down relaxation in mitochondria-rich skeletal muscles. *J Muscle Res Cell Motil* **18**, 473–483.
40 Lee SH, Schwaller B & Neher E (2000) Kinetics of Ca2+ binding to parvalbumin in bovine chromaffin cells: implications for [Ca2+] transients of neuronal dendrites. *J Physiol (Lond)* **525**, 419–432.
41 Collin T, Chat M, Lucas MG, Moreno H, Racay P, Schwaller B, Marty A & Llano I (2005) Developmental changes in parvalbumin regulate presynaptic Ca2+ signaling. *J Neurosci* **25**, 96–107.
42 Izquierdo JM & Cuezva JM (1997) Control of the translational efficiency of beta-F1-ATPase mRNA depends on the regulation of a protein that binds the 3′ untranslated region of the mRNA. *Mol Cell Biol* **17**, 5255–5268.
43 Houstek J, Tvrdik P, Pavelka S & Baudysova M (1991) Low content of mitochondrial ATPase in brown adipose tissue is the result of post-transcriptional regulation. *FEBS Lett* **294**, 191–194.
44 Billups B & Forsythe ID (2002) Presynaptic mitochondrial calcium sequestration influences transmission at mammalian central synapses. *J Neurosci* **22**, 5840–5847.

45 Kirichok Y, Krapivinsky G & Clapham DE (2004) The mitochondrial calcium uniporter is a highly selective ion channel. *Nature* **427**, 360–364.
46 Chin ER, Grange RW, Viau F, Simard AR, Humphries C, Shelton J, Bassel-Duby R, Williams RS & Michel RN (2003) Alterations in slow-twitch muscle phenotype in transgenic mice overexpressing the Ca2+ buffering protein parvalbumin. *J Physiol* **547**, 649–663.
47 Maetzler W, Nitsch C, Bendfeldt K, Racay P, Vollenweider F & Schwaller B (2004) Ectopic parvalbumin expression in mouse forebrain neurons increases excitotoxic injury provoked by ibotenic acid injection into the striatum. *Exp Neurol* **186**, 78–88.
48 Langen H, Roder D, Juranville JF & Fountoulakis M (1997) Effect of protein application mode and acrylamide concentration on the resolution of protein spots separated by two-dimensional gel electrophoresis. *Electrophoresis* **18**, 2085–2090.
49 Chomczynski P & Sacchi N (1987) Single-step method of RNA isolation by acid guanidinium thiocyanate-phenol-chloroform extraction. *Anal Biochem* **162**, 156–159.
50 Bligh EG & Dyer WJ (1959) A rapid method of total lipid extraction and purification. *Can J Biochem Physiol* **37**, 911–917.
51 Rouser G, Fleischer S & Yamamoto A (1970) Two dimensional thin layer chromatographic separation of polar lipids and determination of phospholipids by phosphorus analysis of spots. *Lipids* **5**, 494–496.
52 SAS Institute Inc (1989) *SAS/STAT User's Guide*, version 6, 4th edn. SAS Institute, Cary, NC.